

DynSTGAT: Dynamic Spatial-Temporal Graph Attention Network for Traffic Signal Control

Libing Wu^{1,2,*} Min Wang^{1,2,*} Dan Wu³ Jia Wu⁴

¹School of Computer Science, Wuhan University, Wuhan 430072, China

²State Key Laboratory of Integrated Services Networks, Xidian University, Xi'an 710071, China

³School of Computer Science, University of Windsor, Windsor N9B 3P4, Canada

⁴Department of Computing, Macquarie University, Sydney, NSW 2109, Australia
wu@whu.edu.cn, min.wu@gmail.com, danwu@uwindsor.ca, jia.wu@mq.edu.au

ABSTRACT

Adaptive traffic signal control plays a significant role in the construction of smart cities. This task is challenging because of many essential factors, such as cooperation among neighboring intersections and dynamic traffic scenarios. First, to facilitate cooperation of traffic signals, existing work adopts graph neural networks to incorporate the temporal and spatial influences of the surrounding intersections into the target intersection, where spatial-temporal information is used separately. However, one drawback of these methods is that the spatial-temporal correlations are not adequately exploited to obtain a better control scheme. Second, in a dynamic traffic environment, the historical state of the intersection is also critical for predicting future signal switching. Previous work mainly solves this problem using the current intersection's state, neglecting the fact that traffic flow is continuously changing both spatially and temporally and does not handle the historical state.

In this paper, we propose a novel neural network framework named DynSTGAT, which integrates dynamic historical state into a new spatial-temporal graph attention network to address the above two problems. More specifically, our DynSTGAT model employs a novel multi-head graph attention mechanism, which aims to adequately exploit the joint relations of spatial-temporal information. Then, to efficiently utilize the historical state information of the intersection, we design a sequence model with the temporal convolutional network (TCN) to capture the historical information and further merge it with the spatial information to improve its performance. Extensive experiments conducted in the multi-intersection scenario on synthetic data and real-world data confirm that our method can achieve superior performance in travel time and throughput against the state-of-the-art methods.

KEYWORDS

Reinforcement learning, multi-intersection, traffic signal control, spatial-temporal modeling, graph attention network, temporal convolutional network, intelligent transportation

1 INTRODUCTION

Traffic congestion is one of the problems that everyone often encounters, which has resulted in a waste of people's time. Congestion is caused by many factors, such as the increasing private cars and narrow road structures. However, one of the direct factors is the control of traffic signals. Designing an optimal traffic signal control

scheme can maximize the traffic flow and alleviate transportation congestion. Some traditional methods such as fixed-time control [22] and self-organizing traffic light control [6] can cope with most traffic scenarios. However, they are often inefficient when more vehicles run on the road or the traffic scenarios become complex, especially when there are multiple intersections connected.

Recently, more studies have employed reinforcement learning (RL) to solve the adaptive traffic signal control and achieved promising results [30, 32]. Unlike the conventional heuristic approaches that rely on manually designed rules or the pre-defined traffic flow models, such RL works [4, 31, 33, 37] avoid making pre-defined assumptions and directly learn traffic signal control policies. However, in a multi-intersection scenario, how to collaboratively control traffic signal in a dynamic traffic environment is rarely discussed. First, cooperation among adjacent intersections is essential, especially when they are closely connected since the signal action could affect each other. Second, in dynamic and continuous traffic flow, the signal action is not only related to the current intersection state but also the traffic state at the intersection in the past. If these two challenges are addressed, vehicles will move through intersection quickly, and traffic congestion will be alleviated at the same time.

Some traditional approaches formalize the cooperation among intersections as an optimization problem under certain assumptions. These assumptions, such as uniform vehicle arrival rate [19] and infinite lane capacity [27], do not exist in the real world. When facing today's complex and dynamic traffic flow, our model should be able to cope with various scenarios rather than make more assumptions to limit the applicability of the research.

In a multi-intersection scenario, the most common way to achieve cooperation is to control each intersection with an RL agent. The agents communicate with each other by sharing state information [1, 7–9]. Such RL methods usually take observation s from the target intersection and its neighboring intersections, and then choose an action a to execute. After taking an action, the agent can get a reward r from the environment to evaluate the action through trials and errors, which is a typical and direct way to achieve collaboration, i.e., by expanding the observation scope to obtain more comprehensive information. However, these works [1, 5, 7–9, 26] directly select the state of neighboring intersections and then concatenate them with the target intersection's state, which neglects the fact that traffic flow is changing both spatially and temporally. CoLight [29] is the first to use a graph attention network (GAT) [28] to address the signal cooperation problem among intersections

*Corresponding author.

for large-scale traffic signal control. It models each intersection as a node in graph and learns the dynamic influence of neighboring intersections through graph attention mechanism. As we know, the graph attention network has some advantages in dealing with graph-structured data, but it cannot capture time sequence features. Recently, more variants of spatial-temporal graph neural networks have been widely employed to traffic flow forecasting [36], emotion perception from gaits [24] and point-of-interest recommendation [14]. However, existing RL approaches still do not communicate effectively with neighboring nodes, and no work combines temporal and spatial information for collaborative control. In this paper, we first propose a baseline spatial-temporal graph attention network (STGAT) that adopts the novel multi-head attention mechanism and long short-term memory (LSTM) to facilitate communication of intersections. Instead of directly combining temporal and spatial information, the newly designed STGAT aims to adequately exploit the joint relations of spatial-temporal information by aggregating these information from neighbors.

As mentioned earlier, the adaptive traffic signal control (ATSC) task is challenging because the traffic flow is dynamic and continuous, which means that each intersection state is changing each second. Recently, graph convolutional network [13] or graph attention network [28] are currently making significant progress in the static graph setting, such as graph representation learning [18] and recommendation system [35]. Therefore, if only one graph neural network model is trained for all graphs on the temporal axis, it can hardly learn the changing characteristics of these nodes or intersections. Naturally, more efforts [20, 21, 23] have been made on a dynamic graph like DyRep [23], a two-time scale deep temporal point process model that captures the interleaved dynamics of the observed processes. Moreover, ConSTGAT [10] integrates traffic prediction and contextual information for travel time estimation task. The contextual information of a route, i.e., the connections of adjacent road segments in the route, is an essential factor that affects the driving speed. Despite all this, no one has yet used a dynamic graph neural network in traffic signal control. Inspired by ConSTGAT, in the traffic signal control, an intersection’s contextual information includes the neighboring intersections and its own traffic states in the last time interval of the signal phase. We propose a temporal convolutional network (TCN) [3, 25] to capture the historical state of the target intersection. Then we process the historical information with GAT to get the historical spatial-temporal representation. TCN is a network structure capable of handling time sequence data with parallelism, flexible receptive field, and receiving variable-length inputs compared to LSTM. Considering that vehicles must stop at the intersection when the signal is red, there is no traffic between the two connected intersections. When the signal switches to green, vehicles are moving between them again, i.e., it may take some time for vehicles to arrive from one intersection to another intersection. Therefore, the parallelism and residual module of TCN can help us to overcome this problem.

In this paper, we propose a neural network framework named DynSTGAT, which includes a STGAT model for intersection’s cooperation, a TCN model for sequence feature learning, and a Q-network for action prediction. Specifically, this novel STGAT aggregates information of neighboring intersections, which we call

the current spatial-temporal module. Simultaneously, the combination of TCN and GAT goes for historical state information, which we call the historical spatial-temporal module. Finally, we predict the concatenation of these two modules through a Q-network to obtain the traffic signal action. We experiment on both synthetic and real-world datasets to verify the effectiveness of our method.

In summary, we provide the following three contributions:

- We develop a novel graph neural network framework DynSTGAT for multi-intersection traffic signal control. To the best of our knowledge, we are the first to solve ATSC from the perspective of the dynamic graph based on reinforcement learning.
- The current spatial-temporal module is designed to facilitate cooperation among intersections, and the historical spatial-temporal module is devised to capture historical dynamic state.
- We conduct extensive experiments on both synthetic and real-world datasets, which demonstrates that our method can significantly outperform the state-of-the-art methods.

2 RELATED WORK

This section discusses three types of works closely related to our research: traffic signal control, graph attention network, and temporal convolutional network.

2.1 Traffic Signal Control

Adaptive traffic signal control (ATSC) can be divided into two types: individual traffic signal control and multi-intersection traffic signal control. This paper focuses on signal control in multi-intersection scenarios [30]. The final purpose of ATSC is to shorten the total vehicle travel time or reduce the waiting time of vehicles when crossing the intersection by optimizing the signal switching. In a multi-intersection scenario, the cooperation between the connected intersections is essential, and many existing RL-based studies [1, 5, 7–9, 26] expand the scope of observation and then concatenate them together. This approach treats the neighboring intersections equally, which is incorrect because the traffic is changing continuously. To address this problem, we leverage DynSTGAT to continuously obtain the dynamics of neighboring intersections, including the current and historical spatial-temporal information. In summary, the proposed framework DynSTGAT can benefit from cooperation and dynamic influence of the surrounding intersections.

2.2 Graph Attention Network

Graph neural network (GNN) such as GCN and GAT have recently achieved overwhelming results in computer vision, recommendation system, social network, and other areas employing graph structures. The introduction of GNN has motivated the following works to employ the spatial-temporal graph neural network (STGNN) on traffic forecasting [12, 15, 36]. Compared to GNN, STGNN utilizes both temporal and spatial information. Typically, STGNN uses GCN or GAT to capture structural or geographic information and then uses LSTM to obtain temporal information. Although many previous works have applied STGNN, most of them only fuse these two independent features without considering their joint relations. Considering that GAT has proven effective in CoLight [29], we first propose a new spatial-temporal graph attention network (STGAT)

to adequately exploit the structural and temporal information simultaneously. We also handle dynamic historical spatial-temporal information on this basis and then concatenate it with current spatial-temporal information to form the final DynSTGAT.

2.3 Temporal Convolutional Network

As we know, GRU and LSTM are current first solutions to solve the sequence problems, but many variants of LSTM do not have a significant improvement over the standard LSTM. Besides, GRU and LSTM cannot perform massive parallel processing like CNN. The temporal convolutional network [3, 25] is a brand-new neural network architecture that can solve time sequence problems, and it combines both dilated convolution and causal convolution structures. Compared to LSTM, it has parallelism, flexible receptive fields, and receives variable-length inputs. What is more, temporal convolutional network (TCN) is smaller in size and less time-consuming than RNN. It is also widely used in tasks such as human trajectory prediction [16] and action segmentation [11]. We are inspired by TCN and then use it to obtain historical state temporal representation of the target intersection. This temporal representation combined with the spatial relations of neighboring intersections forms the historical spatial-temporal representation. Neighboring intersections are those intersections that are directly connected to the target intersection. More details about the usage of TCN and spatial-temporal information are discussed in section 4.

3 PROBLEM DEFINITION

3.1 Preliminaries

In this paper, we investigate the multi-intersection traffic signal control. To illustrate the intersection definition in detail, we only take one intersection shown in Figure 1 as an example. A multi-intersection scenario is composed of multiple such single intersections connected.

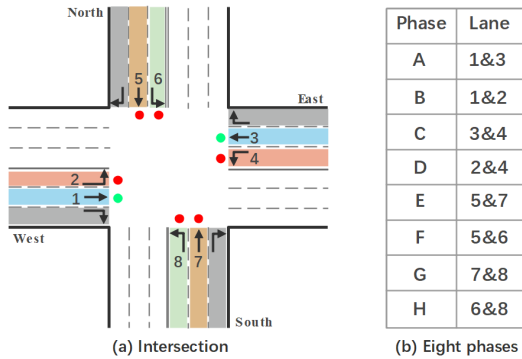


Figure 1: The illustration of an intersection with 8 phases. The number marked in the figure(a)(b) is the entering lane.

Intersection. Each intersection has four entering approaches (East, West, South and North), and each entering approach has three lanes. As shown in Figure 1(a), a left-turn lane, a straight lane, and a right-turn lane compose the approach. The rightmost lane of intersection is not set with a traffic signal.

Traffic movement. We define a traffic movement as the traffic moving through an intersection, i.e., left-turn, straight, and right-turn. We define a traffic movement from lane l to lane m as (l, m) ,

in Figure 1(a), there are total 12 traffic movements¹. In addition, a traffic movement can occupy more than one lane since a traffic signal controls a traffic movement rather than a lane.

Phase setting. A traffic signal phase p is defined as a set of permissible traffic movements. As shown in Figure 1(b), this intersection has 8 phases, where phase ‘A’ is activated and it can be vectorized as $\vec{p} = [1, 0, 0, 0, 0, 0, 0, 0]$. Each element in the one-hot vector \vec{p} represents a traffic signal. In this case, vehicles in East and West cross lanes can go straight to the corresponding exiting lanes.

Pressure of each signal phase. For each signal phase p , there are several permissible traffic movements (l, m) . We denote $d(l, m)$ with the difference in the number of vehicles on lane l and lane m . Therefore, the pressure of a signal phase p is the total sum of the pressure of its permissible phases $\sum_{(l, m)} d(l, m), \forall (l, m) \in p$.

Pressure of an intersection. The intersection pressure P_i is the difference between the sum of all queued vehicles on entering lanes and the sum of all queued vehicles on exiting lanes. As shown in Figure 2, the pressure of the middle intersection is 7, where the orange-pink part is the entering lanes, and the blue part is the exiting lanes.

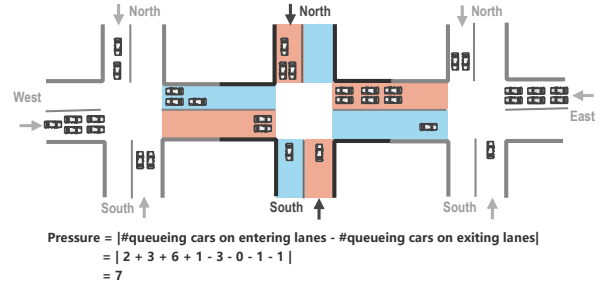


Figure 2: The illustration of intersection pressure.

3.2 RL Environment

We leverage reinforcement learning to model signal control, where reinforcement learning consists of an environment and an agent. Each intersection is controlled by an agent. The environment and the agent continuously interact to maximize the reward in the long run through trial and error. The traffic signal control problem can be formulated as a typical Markov Decision Process $\langle S, \mathcal{A}, \mathcal{P}, r, \gamma \rangle$.

- State space S . Each intersection I_i can observe its own state s_i^t at time t . In this work, we define the state of an intersection with its current phase \vec{p} and the number of vehicles \vec{n} on each lane at the intersection, i.e., $s_i^t = [\vec{p}, \vec{n}]$. For a standard intersection with 12 traffic movements or lanes, the length of \vec{n} is 12.
- Action set \mathcal{A} . Each agent takes a phase p as its action a_i^t at time t . Note that not all eight signal phases are selected. The RL algorithm selects only one of them at each step. We set the execution time of each action $\Delta t = 10s$, which is the green time of phase. The yellow time of phase $t_y = 3s$ is designed to let the remaining vehicles all leave the intersection.
- Transition probability \mathcal{P} . At time t , it represents the probability $\mathcal{P}(s_i^{t+1} | s_i^t, a_i^t)$ when the intersection or environment changes from one state s_i^t to the next state s_i^{t+1} .

¹In this paper, we only consider no more than 12 traffic movements, but the proposed method can be extended to control intersections with more than 12 movements.

- Reward r measures the feedback from environment after agent i taking action a_i^t . In Figure 2, we define the reward r_i for agent i as the pressure on the intersection, which is the difference between the sum of all queued vehicles on entering lanes and the sum of all queued vehicles on exiting lanes. If we represent the pressure of intersection I_i with P_i , then the system reward r_i should be

$$r_i = -P_i \quad (1)$$

By maximizing reward, agent can understand which action has positive feedback or negative feedback to learn the environment better and let vehicles cross the intersection more quickly.

- Discount factor γ . At time t , the agent chooses an action to execute, and its goal is to maximize the total reward $G_i^t = \sum_{t=\tau}^T \gamma^{t-\tau} r_i^t$, where T is the total time of one episode and $\gamma \in [0, 1]$ differentiates the immediate reward and future reward.

In this work, we adopt the action-value function Q to approximate the total reward G_i^t with our DynSTGAT. Therefore the loss function of the Q-network can be defined as follows:

$$\mathcal{L}(\theta) = \mathbb{E}[(r_i^t + \gamma \max_{a'} Q(s_i^t, a'; \theta') - Q(s_i^t, a_i^t; \theta))^2] \quad (2)$$

where s_i^t, a_i^t is the next state and next action, and θ, θ' are all trainable parameters in model.

4 METHOD

In this part, we detail the proposed dynamic spatial-temporal graph attention network based on reinforcement learning.

4.1 Framework

Figure 3 plots the architecture of the our framework DynSTGAT, which consists of four modules: current spatial-temporal module, historical or dynamic spatial-temporal module, spatial module, and integration module. The current spatial-temporal module combines a novel spatial-temporal graph attention network and LSTM to capture the joint relations of temporal and spatial information of the current traffic state. The historical spatial-temporal module utilizes a novel spatial-temporal graph attention network and TCN to capture the joint relations of temporal and spatial information of the historical traffic state. The spatial module also uses a graph network to obtain spatial relations. The integration module takes a Q-network to predict the concatenation of two types of spatial-temporal information and generate each phase's action.

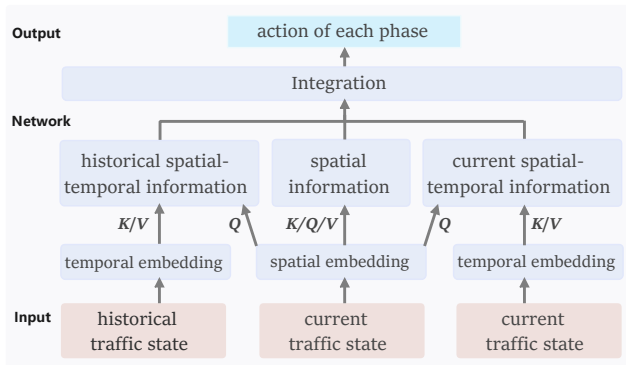


Figure 3: The architecture of DynSTGAT, where K, Q, V denotes keys, query, and values in the attention mechanism.

4.2 State Embedding

At time t , after getting a state from the intersection I_i , i.e., the number of vehicles runs on each lane and the current signal phase, we first employ two layers of Multi-Layer Perceptron (MLP) to embed the d_0 -dimensional state s_i^t into d_1 -dimensional latent space:

$$\begin{aligned} h_0 &= \text{Dense}(s_i^t) = \sigma(s_i^t W_e^{11} + b_e^{11}) \\ h_i &= \text{Dense}(h_0) = \sigma(h_0 W_e^{21} + b_e^{21}) \end{aligned} \quad (3)$$

where $s_i^t \in \mathbb{R}^{d_0}$ is the state of intersection I_i at time t and d_0 is the feature vector dimension of s_i^t , $W_e^{11} \in \mathbb{R}^{d_0 \times d_1}$, $W_e^{21} \in \mathbb{R}^{d_1 \times d_1}$ and $b_e^{11}, b_e^{21} \in \mathbb{R}^{d_1}$ are weight matrix and bias vector when training. **Dense** is a fully-connected layer and σ is the ReLU activation function. The generated hidden state $h_i \in \mathbb{R}^{d_1}$ denotes the current traffic condition of i -th intersection. Note that h_i is used to capture current temporal information, as shown in Figure 4.

Similarly, we use another two layers of Multi-Layer Perceptron to encode the current state so that it can be used to obtain spatial information. As shown in Eq. (4), $W_e^{12} \in \mathbb{R}^{d_0 \times d_1}$, $W_e^{22} \in \mathbb{R}^{d_1 \times d_1}$ and $b_e^{12}, b_e^{22} \in \mathbb{R}^{d_1}$ are weight matrix and bias vector when training.

$$\begin{aligned} \hat{h}_0 &= \text{Dense}(s_i^t) = \sigma(s_i^t W_e^{12} + b_e^{12}) \\ h_j &= \text{Dense}(\hat{h}_0) = \sigma(\hat{h}_0 W_e^{22} + b_e^{22}) \end{aligned} \quad (4)$$

4.3 Current Spatial-Temporal Module

The traffic conditions at an intersection are strongly correlated with the current conditions itself and its neighboring intersections. For example, traffic congestion at one intersection may have a high probability of causing traffic congestion on its neighboring intersections within a short time. To the best of our knowledge, CoLight [29] summarize the geographic effect of connected intersections, and it does not take temporal information into account. Besides, although the spatial-temporal graph neural network is widely adopted, temporal and spatial information is used separately. To take full advantage of the joint relations of temporal and spatial information, we develop a novel spatial-temporal graph attention network, where GAT is used to capture spatial information and LSTM is used to deal with the current temporal information, respectively.

We introduced in detail the novel attention mechanism for capturing the spatial-temporal relations of traffic states, which is an extension of graph attention network [28], as shown in Figure 4.

First, we embed the current state s_i^t into a latent space and get the hidden representation h_i and h_j . Then we encode the hidden representation h_i with LSTM to get the current temporal information x_i , as defined in Eq. (5), where $cstate$ and $hstate$ are the initial cell state and hidden state in LSTM. x_c and x_h are the cell state and hidden state at the last step. We set the 'return_sequences' parameter to true, so that x_i represents a time sequence tensor.

$$x_i, x_c, x_h = \text{LSTM}(h_i, cstate, hstate) \quad (5)$$

$$Q_i = h_j, \quad K_i = x_i, \quad V_i = x_i \quad (6)$$

Next, we use the attention mechanism [2] to learn the cooperation between intersections and capture the joint relations of current spatial-temporal information. Then the target intersection can get the overall influence of the surrounding intersections. Specifically, as defined in Eq. (6), the generated hidden representation h_j is taken

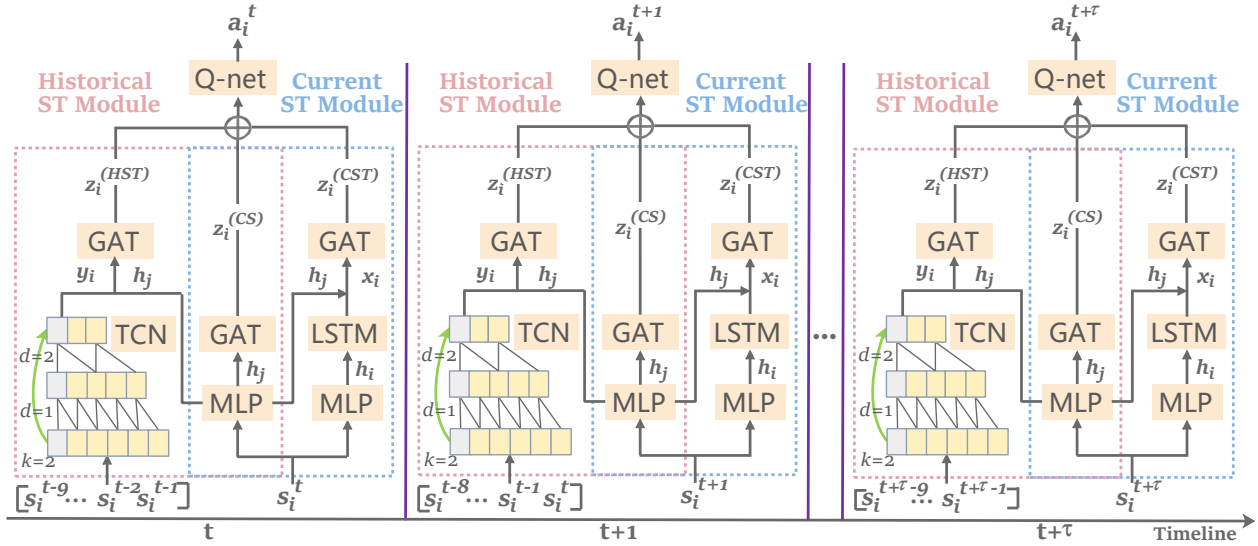


Figure 4: An illustration of the proposed dynamic spatial-temporal graph attention network framework-DynSTGAT. ST stands for spatial-temporal, and in the later experiments, we set the dilation factors $d=1, 2, 4, 8$ and kernel size $k=2$ in TCN.

as the *query* of the attention mechanism. The current temporal information x_i is taken as *keys* and *values* of the attention mechanism. To be specific, the novel attention mechanism is defined as:

$$f(Q_i, K_{i,u}) = \frac{Q_i \cdot K_{i,u}}{\sqrt{d^{(H)}}} \quad (7)$$

$$\alpha(Q_i, K_{i,u}) = \frac{\exp(f(Q_i, K_{i,u}))}{\sum_{u' \in \mathcal{NB}_i} \exp(f(Q_i, K_{i,u'}))} \quad (8)$$

$$Attention^{(1)}(Q_i, K_i, V_i) = \frac{1}{He} \sum_{h=1}^{h=He} \sum_u \alpha(Q_i, K_{i,u}) V_{i,u} \quad (9)$$

Where $d^{(H)}$ is the hidden size of attention mechanism, $u \in \mathcal{NB}_i$ and \mathcal{NB}_i is the neighboring intersections of the target intersection I_i , He is the number of attention heads. The first step is to calculate the scaled dot $f(Q_i, K_{i,u})$ of *query* and *key*, as shown in Eq. (7). Then the attention scores $\alpha(Q_i, K_{i,u})$ is obtained by the *softmax* activation function. Finally, the relations between *query* and the current intersection's state can be encoded as:

$$z_i^{(CST)} = Attention^{(1)}(Q_i, K_i, V_i) \quad (10)$$

Compared with other existing spatial-temporal graph neural networks, our attention mechanism is elaborately designed to adequately exploit joint relations of spatial-temporal information. This mechanism can also be employed to other spatial-temporal problems.

4.4 Current Spatial Module

In the subsection 4.3, we computed the current spatial-temporal information representation $z_i^{(CST)}$ by treating h_j as *query*. In the same way, we can simultaneously take h_j as *query*, *keys*, and *values* to compute spatial representation $z_i^{(CS)}$, as defined in Eq. (11). Three calculation formulas here are the same as Eq. (7)(8)(9), so we omit

them and directly give the final spatial representation.

$$\begin{aligned} Q_i^{(2)} &= h_j, & K_i^{(2)} &= h_j, & V_i^{(2)} &= h_j \\ & & & \dots & & \\ z_i^{(CS)} &= Attention^{(2)}(Q_i^{(2)}, K_i^{(2)}, V_i^{(2)}) \end{aligned} \quad (11)$$

Since the topology of the multi-intersection is fixed, we only characterize the spatial dependencies at the current moment. With this novel attention mechanism, the target intersection can generate the overall influence summary of its neighboring intersections.

4.5 Historical Spatial-Temporal Module

The switching of an intersection's signal is closely related to the traffic conditions at the current moment and the historical state, such as state during the last green time interval. To the best of our knowledge, the traffic flow is continuous, so historical traffic conditions are critical. In contrast, this has not been considered in previous work. Due to the traffic lights set at the intersection, only a part of the traffic movement has cars passing each step, which means that the number of cars in the other lanes may remain the same. In the temporal dimension, a problem arises about capturing such features in discontinuous changes in the number of vehicles. Inspired by the temporal convolutional network [3], we take advantage of its flexible receptive field and other properties to capture the dynamic features in green time of the last signal phase.

Specifically, we first collect the historical state of intersection I_i during the green time of the last signal phase. We set the green time to 10 seconds, so the historical state at time t can be denoted as $D_i = [s_i^{t-9}, \dots, s_i^{t-2}, s_i^{t-1}]$. Then we encode the historical or dynamic state D_i by two layers of TCN network, as shown in Eq. (12). Each TCN layer consists of one residual block and four hidden layers, and the corresponding dilation factors of the four hidden layers are 1, 2, 4, 8, as shown in Figure 5. We can sum the tensor of the four hidden layers and get the final output O_i^0, O_i^1 by linear

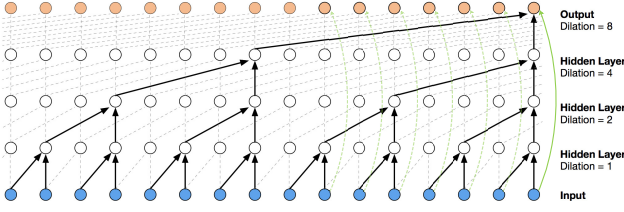


Figure 5: Stack of dilated causal convolutional layers and residual connection in our temporal convolutional network.

transformation with one ReLU activation layer.

$$O_i^0 = \text{TCN}(D_i) \quad (12)$$

$$O_i^1 = \text{TCN}(O_i^0)$$

$$\hat{Y}_i = \text{GlobalMaxPooling}(O_i^1) \quad (13)$$

$$\bar{Y}_i = \text{GlobalAveragePooling}(O_i^1)$$

$$y_i = \text{Dense}(\text{Concat}(\hat{Y}_i, \bar{Y}_i)) \quad (14)$$

Next, we perform global average pooling and global maximum pooling transformations on the time series tensor O_i^1 , as shown in Eq. (13). These two pooling operations can reduce the computational cost by sampling the tensor, i.e., downsampling a large tensor into a small one, which can prevent overfitting at the same time. Finally, we concatenate the pooling results \hat{Y}_i, \bar{Y}_i and encode them with a **Dense** layer to generate the temporal representation y_i , as shown in Eq. (14). This temporal feature includes the dynamic changes of the target intersection’s state during the green time of the previous signal phase, which is essential for predicting the current phase.

Same as in subsection 4.3, we can employ the new attention mechanism to fuse this historical temporal and spatial information. Similarly, we take the hidden representation h_j as *query*, and then take the historical or dynamic temporal information y_i as *keys* and *values*. After representing $Q_i^{(3)}, K_i^{(3)}, V_i^{(3)}$, the next step is to calculate the attention scores and the multi-head attention summation. As shown in Eq. (15), three formulas here are the same as Eq. (7)(8)(9), so we omit these three calculation equations.

$$\begin{aligned} Q_i^{(3)} &= h_j, & K_i^{(3)} &= y_i, & V_i^{(3)} &= y_i \\ & \dots & & & & \\ z_i^{(HST)} &= \text{Attention}^{(3)}(Q_i^{(3)}, K_i^{(3)}, V_i^{(3)}) \end{aligned} \quad (15)$$

Compared with the other studies, we deal with the historical state of the intersection for the first time and combine it with spatial information to form the historical or dynamic spatial-temporal representation. The following subsection will elaborate how to predict the target intersection’s signal action with these spatial-temporal information $z_i^{(CST)}, z_i^{(CS)}$ and $z_i^{(HST)}$.

4.6 Q-value Prediction

As illustrated in Figure 4, the last part of the DynSTGAT model is to predict the action of intersection through a Q-network. Specifically, the Q-network is used to predict the Q-value $\bar{q}(o_i^t)$ corresponding to each permissible action, as defined in Eq. (16). Then the signal action a_i^t can be decided based on the maximum Q-value.

$$\bar{q}(o_i^t) = \text{Dense}(\text{Concat}(z_i^{(CST)}, z_i^{(CS)}, z_i^{(HST)})) \quad (16)$$

Table 1: Four configurations of synthetic traffic dataset.

Config	Demand Pattern	Arrival rate (vehicles/s)
1	Flat	0.388
2	Peak	
3	Flat	0.416
4	Peak	

According to the pre-defined loss function Eq. (2), we can update the loss function for our DynSTGAT as follows:

$$\mathcal{L}(\theta) = \frac{1}{T} \sum_{t=1}^T \sum_{i=1}^N (q(o_i^t, a_i^t) - \bar{q}(o_i^t, a_i^t; \theta))^2 \quad (17)$$

where T is the total time steps at each episode, N is the total number of intersections in the road network, and θ denotes all the trainable parameters in DynSTGAT. From the perspective of each intersection, its state and the state of neighboring intersections are changing. Our proposed newly graph attention mechanism can capture these dynamic changes from both temporal and spatial dimensions. In other words, DynSTGAT can address both cooperation and dynamism problems in adaptive traffic signal control.

4.7 Overall Architecture

The overall architecture of the proposed DynSTGAT model is illustrated in Figure 4. It mainly contains a historical spatial-temporal (ST) module marked by pink dashed box and a current spatial-temporal (ST) module marked by blue dashed box, which shares an intermediate spatial module. Although GAT is shown in the figure, as mentioned earlier, the novel attention mechanism we employ is an extension of the original GAT. Note that the output of Q-network is the Q-value of each action, and we can select action a_i^t to execute by agent based on the maximum Q-value.

5 EXPERIMENTS

We conduct experiments on one synthetic dataset and two real-world datasets to verify and evaluate our proposed method.

5.1 Settings

We experiment on an open-source traffic simulator CityFlow², which provides a set of rich interface functions and supports large-scale city traffic signal control [34]. The intersection’s state can be subscribed from the simulator, and the simulator can execute traffic signals according to the selected phases.

Experiment settings: We set the simulation time to 1800s for the synthetic dataset and 3600s for the real-world dataset. The total number of training rounds or episodes is 200, and the synthetic dataset is a 4×4 road network. To ensure training data diversity, we parallel run three processes on the same road network during training. **Agent settings:** We set the batch size to 20, discount factor $\gamma=0.8$, and the training epoch is 100 for each round. The total length of experience replay memory is 10000, and the sampling size is 1000. **Traffic environment settings:** We set the green time to 10s and followed by yellow time 3s and red time 2s. The number of neighboring intersections is 4.

²<https://cityflow-project.github.io>

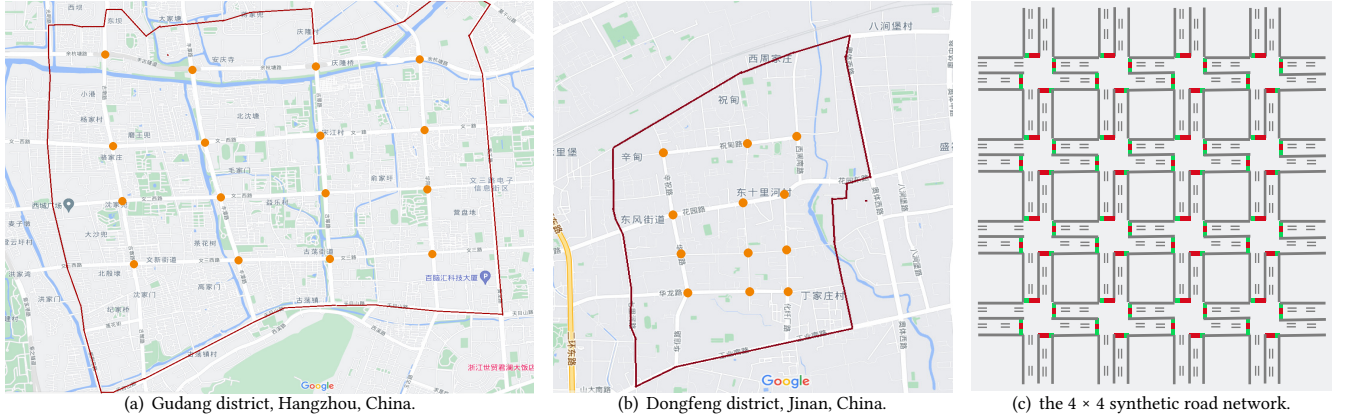


Figure 6: Road networks for real-world datasets (a)(b) and synthetic dataset (c). In the Hangzhou and Jinan road networks, red polygons are the areas we chose to model, and yellow dots are the traffic signals we control. In the synthetic road network, each standard intersection has 12 traffic movements, as shown in Figure 1. Hangzhou (a): 16 intersections with uni- & bi-directional traffic, Jinan (b): 12 intersections with bi-directional traffic, 4 × 4 synthetic grid (c): 16 intersections with bi-directional traffic.

Table 2: Data statistics of the real-world traffic datasets.

Dataset	#intersections	Arrival rate (vehicles/300s)			
		Mean	Std	Max	Min
$D_{Hangzhou}$	16	526.63	86.70	676	256
D_{Jinan}	12	250.70	38.21	335	208

5.2 Datasets

We experiment with two real-world datasets and one synthetic dataset with four different configurations. The real-world datasets are collected from Hangzhou and Jinan in China. In these traffic datasets, each vehicle is recorded as (o, t, d) where o is origin road, t means departure time, and d is the destination road. All data have been converted into *JSON* format, and we only need to import road files and traffic flow files in the simulator to run these data directly.

• **Synthetic dataset** road network is shown in Figure 6(c), where each intersection has four entering approaches with 300-meter long road segments. As listed in Table 1, we use four configurations to test the signal control models in different traffic demands: two types of vehicles’ average arriving rate, each with Flat (0.3 variance) and Peak (0.6 variance) patterns. All the vehicles enter and leave the road network at the rim edges. The turning ratios at the intersection are set as 10% (left), 60% (straight), and 30% (right) based on the statistical analysis on real-world datasets.

• **Real-world datasets** Hangzhou and Jinan were collected from intersection surveillance cameras rather than going to real-world intersections to conduct experiments. Their road networks are shown in Figure 6(a)(b), and we list the traffic flow statistics in Table 2, which are processed from several sources. More details about the processing of the two datasets are shown below:

$D_{Hangzhou}$: There are 16 intersections selected to model in Gudang district, Hangzhou, China, as illustrated in Figure 6(a). The surveillance records in the dataset include time, camera ID and vehicle information. After analyzing and pre-processing these records and camera positions, the trajectories of vehicle are recorded when they move through the intersections. To facilitate the simulation, we

will count the number of vehicles crossing intersections and use it as the traffic volume in experiments.

D_{Jinan} : Similar to Hangzhou, this dataset includes 12 intersections in Dongfeng district, Jinan, China, as shown in Figure 6(b).

5.3 Compared Methods

In order to evaluate the effectiveness and efficiency of our proposed method, we compare it with the following conventional and best optimal RL-based methods. For a fair comparison, all RL models are trained from scratch and without any pre-training, and we report the final results as the average of the last ten episodes of testing.

- **FixedTime** [22]. The fixed-time control method needs to pre-design a fixed cycle length and signal phase time rules, which are mainly adapted to relatively steady traffic flow.
- **NeighborRL** [1]. This is a multi-agent deep Q-learning algorithm that allows agent to incorporate their neighboring intersections’ traffic state with their own for cooperation.
- **GRL** [26]. An RL-based method for coordinating the multi-agent traffic signal control. Specifically, transfer planning and maximum coordination algorithm are employed to the coordination.
- **GCN** [17]. This is an RL-based traffic signal control method that employs graph convolutional network (GCN) automatically to obtain the geometric features among multi-intersection.
- **CoLight** [29]. Graph attention network (GAT) is adopted to enhance spatial communication among the neighboring intersections. It is scalable for network-level multi-agent traffic signal control.
- **STGAT**. This is our baseline for traffic signal control with spatial-temporal graph attention network. It differs from DynSTGAT in that it only models the traffic condition at the current moment, including both temporal and spatial information.
- **DynSTGAT**. The neighborhood scope of the intersection is designed by the node distance, i.e., the minimum number of hops between two connected intersections.
- **DynSTGAT-geo**. It shows that the neighborhood scope of the intersection is measured by the road or geographical distance.

5.4 Evaluation Metric

We select the following two representative measures to evaluate different methods, which are the most frequently used metrics to judge the performance of traffic signal control [30].

- **Travel time.** This metric describes the average time that all the vehicle spends on the lanes (in seconds). For those vehicles that complete the trips from the starting road to the ending road, we define the travel time as to the difference between the vehicle’s time at starting road and vehicle’s time at the ending road. As for the rest of the vehicles that have not reached the destination when the simulation time is over, they are not counted in the final results. A shorter travel time means the vehicle completes its trip in a shorter time, indicating better model performance.
- **Throughput.** It represents the number of vehicles that finished the trip during the whole simulation. A larger throughput in the given period means more vehicles completed their trips, indicating a better control strategy.

5.5 Performance Evaluation

5.5.1 Overall Analysis. We report travel time and throughput of the proposed DynSTGAT, traditional methods, and state-of-the-art RL-based methods on synthetic datasets and real-world datasets in Table 3 and Table 4. We can get the following observations:

1. In Table 3, the proposed DynSTGAT outperforms all the other methods in the four different synthetic configurations, delivering the least travel time and the maximum throughput. The maximum improvement in travel time is 13.8% over the first optimal solution CoLight under Config 2, while the maximum enhancement of throughput over CoLight is as high as 25.9% under Config 3. The advantage of DynSTGAT over other traditional and RL methods is attributed to its elaborately reward designed and direct feedback on how well the agent learns. In other words, DynSTGAT optimizes the control policy by reducing the pressure between the entering and exiting lanes. Compared with the other graph-level methods such as CoLight and STGAT, DynSTGAT makes full use of temporal and spatial information with the novel attention mechanism. Although STGAT can achieve relatively good results, it ignores the impact of the traffic conditions during the last green time interval.

2. Table 4 lists the performance on real-world datasets Hangzhou and Jinan. Specifically, general reinforcement learning methods such as NeighborRL and GRL are even inferior to traditional method FixedTime. The main reason for this is that these two methods take the state of the neighboring intersections as their own observable state, ignoring the spatial correlation between them. The graph network based approaches are better than the previous three approaches. Explicitly, our three models STGAT, DynSTGAT, and DynSTGAT-geo, all perform better than the other methods. The travel time of DynSTGAT-geo is improved by 7.2% and 3.6% over CoLight on the Hangzhou and Jinan datasets, respectively. On the real-world dataset, the distances of neighboring intersections are not equal, so it is reasonable to use geographic distance to represent the neighborhood scope of an intersection. The throughput of the last four graph methods is 2974 on Hangzhou dataset because the simulation time in this dataset is 3600s, and the total number of vehicles is 2984. Within this simulation time, almost all the vehicles

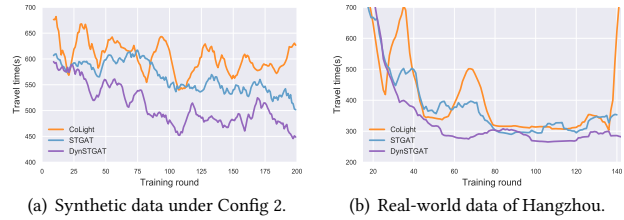


Figure 7: Convergence speed of DynSTGAT (purple continuous curves) and other two graph methods during training.

can reach the destination and complete the trip. On Jinan dataset, the simulation time is 3600s, and the number of vehicles is 6296.

3. When comparing the performance of the proposed DynSTGAT with the traditional method FixedTime, we find the travel time gap becomes more prominent as the tested data varies from regular synthetic traffic (average gap 13.3%) to real-world dynamic changing traffic (average gap 64.4%). This growing performance difference is consistent with FixedTime’s inherent flaw, namely its inability to learn from the feedback of the environment.

5.5.2 Convergence Speed Comparison. We plot DynSTGAT’s performance curve of average travel time in each round or episode, and then compare it with the other two graph-based methods, as shown in Figure 7. Evaluated on the two representative datasets, DynSTGAT performs better than the other two methods in terms of fast convergence rate and travel time at stabilization. Figure 7(a) depicts DynSTGAT consistently has lower travel time than the other two methods, while in Figure 7(b), DynSTGAT converges faster than the other two methods, having converged about 60 rounds. Learning the spatial-temporal information on neighborhood does not slow down the convergence of model or affect the smoothness when the model reaches stability.

5.6 Study of DynSTGAT

5.6.1 Effectiveness. As reported in Tables 3, 4 and the convergence curve in Figure 7, DynSTGAT consistently outperforms other methods on synthetic grid road and the real-world road. In fact, DynSTGAT is scalable to any road network as long as the distances to neighboring intersections are measurable.

5.6.2 Impact of Neighborhood Definition. The neighborhood scope of an intersection has the following two definition ways, road distance and node distance. The road distance denotes the actual distance between the geographical location of two intersections, and node distance is the minimum hop number between two nodes, where each node is an intersection in the road network. The results reported in Table 4 prove that DynSTGAT using geographical distance delivers higher performance than that using node distance. Considering that the connected intersections in the synthetic road network are equidistant, we only compare DynSTGAT with other methods instead of DynSTGAT-geo.

5.6.3 Impact of Parameter Sharing. To study the effect of parameter sharing on model learning, we compare the number of rounds for the model to converge with and without parameter sharing under synthetic traffic. As shown in Figure 8, parameter sharing allows our

Table 3: Performances of different methods evaluated on the four configurations of synthetic dataset. For average travel time, the lower the better. Travel time is reported in second. For throughput, the higher the better. Same with the following table.

Model	Travel Time				Throughput			
	Config 1	Config 2	Config 3	Config 4	Config 1	Config 2	Config 3	Config 4
FixedTime[22]	573.1	564.0	536.0	563.1	3555	3477	3898	3556
NeighborRL[1]	690.9	687.3	781.2	791.4	3504	3255	2863	2537
GRL[26]	735.4	758.6	771.1	721.4	3122	2792	2962	2991
GCN[17]	516.7	523.8	646.2	585.9	4275	4151	3660	3695
CoLight[29]	515.9	517.0	553.4	524.3	4206	3480	3853	3891
STGAT	513.4	501.7	539.0	516.8	4823	4152	4577	4218
DynSTGAT	471.9	445.6	519.0	500.1	5003	4312	4852	4265

Table 4: Performance comparison on real-world datasets.
*No result reported in throughput because we want to compare our method with the graph-level attention method.

Model	Travel Time		Throughput	
	Hangzhou	Jinan	Hangzhou	Jinan
FixedTime[22]	728.8	869.9	—*	—*
NeighborRL[1]	1053.5	1168.3	—*	—*
GRL[26]	1582.3	1210.7	—*	—*
GCN[17]	768.4	625.7	—*	—*
CoLight[29]	303.5	294.0	2974	5513
STGAT	289.1	305.8	2974	5420
DynSTGAT	286.5	287.6	2974	5572
DynSTGAT-geo	281.5	283.3	2974	5604

model to converge faster, verifying the effectiveness of parameter sharing for traffic signal control in multi-intersection scenarios.

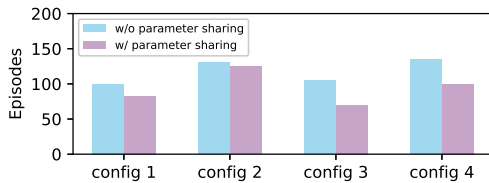


Figure 8: Number of episodes for model to converge.

5.6.4 Impact of Neighbor Number. Figure 9(a) plots the performance of DynSTGAT affected by different number of neighbors under different training rounds. When the number of neighbors increases from 2 to 5, DynSTGAT achieves the optimal performance. Too many neighbors require more training time (200 episodes) to learn relations between intersections. Therefore, considering the impact of the four nearby intersections on the target intersection appears sufficient to guarantee performance for traffic signal control.

5.6.5 Impact of Attention Head Number. To investigate the impact of multi-head attention on model performance, we test and verify two models STGAT and DynSTGAT on dataset $D_{Hangzhou}$. As shown in Figure 9(b), we can observe that as the numbers of attention heads increase, less travel time is spent on road networks. However, when the attention head parameter He exceeds 5, the advantage of multi-head attention gradually disappears. We can

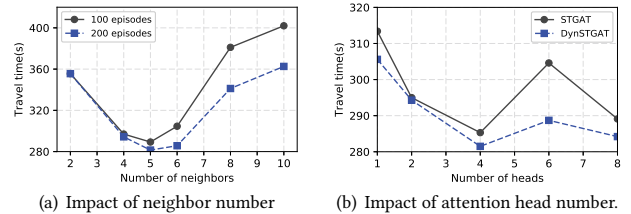


Figure 9: Performance of DynSTGAT with different number of neighbors on $D_{Hangzhou}$ (a). Performance comparison with different number of attention heads on $D_{Hangzhou}$ (b).

draw the same conclusions in other datasets, not all shown due to space limitation.

6 ATTENTION STUDY

The left part of Figure 10 displays a target intersection (the green dot) in the Hangzhou dataset, whose neighborhood has two vertical intersections (**A**, **B**) and two arterial intersections (**C**, **D**). The horizontal arterial street is uni-directional, and the traffic flow is high, while the longitudinal side street is bi-directional, and the traffic flow is low. The right part of Figure 10 plots the attention score distribution (blue and yellow lines) can observe that the arterial intersections (red and purple lines). The target intersection has the largest self-attention score (green line), indicating that the traffic state at this intersection is more critical at the current moment.

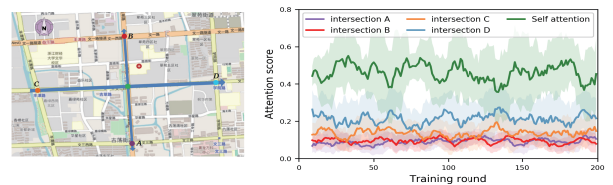


Figure 10: A typical intersection with its neighbors and spatial attention scores learned by DynSTGAT when training.

7 CONCLUSION

In this work, we develop a well-designed graph neural network framework DynSTGAT based on reinforcement learning to address the multi-intersection traffic signal control problem. Specifically, our current spatial-temporal module can learn the dynamic communication or cooperation between intersections, and the historical

spatial-temporal module can learn the dynamic changes of traffic condition on the target intersection. In addition, we design a novel graph attention mechanism, which is an extension of GAT and can help us adequately exploit the joint relations of spatial-temporal information. Extensive experiments conducted on both synthetic and real-world datasets confirm the effectiveness and efficiency of our proposed method than the state-of-the-art methods.

For future work, we will attempt to investigate the traffic scenarios with dozens or even hundreds of intersections or scenarios with more complex road designs. In addition, the neighborhood scope of an intersection should be various, for example, incorporating second-order and even higher-order neighboring intersection.

REFERENCES

- [1] Itamar Arel, Cong Liu, Tom Urbanik, and Airton G Kohls. 2010. Reinforcement learning-based multi-agent system for network traffic signal control. *IET Intelligent Transport Systems* 4, 2 (2010), 128–135.
- [2] Dzmitry Bahdanau, Kyunghyun Cho, and Yoshua Bengio. 2014. Neural machine translation by jointly learning to align and translate. *arXiv preprint arXiv:1409.0473* (2014).
- [3] Shaojie Bai, J Zico Kolter, and Vladlen Koltun. 2018. An empirical evaluation of generic convolutional and recurrent networks for sequence modeling. *arXiv preprint arXiv:1803.01271* (2018).
- [4] Chacha Chen, Hua Wei, Nan Xu, Guanjie Zheng, Ming Yang, Yuanhao Xiong, Kai Xu, and Zhenhui Li. 2020. Toward A thousand lights: Decentralized deep reinforcement learning for large-scale traffic signal control. In *Proceedings of the AAAI Conference on Artificial Intelligence*, Vol. 34. 3414–3421.
- [5] Tianshu Chu, Jie Wang, Lara Codecà, and Zhaojian Li. 2019. Multi-agent deep reinforcement learning for large-scale traffic signal control. *IEEE Trans. Intelligent Transportation Systems* 21, 3 (2019), 1086–1095.
- [6] Seung-Bae Cools, Carlos Gershenson, and Bart D’Hooghe. 2013. Self-organizing traffic lights: A realistic simulation. In *Advances in applied self-organizing systems*. Springer, 45–55.
- [7] Bruno C Da Silva, Eduardo W Basso, Filipo S Perotto, Ana L C. Bazzan, and Paulo M Engel. 2006. Improving reinforcement learning with context detection. In *Proceedings of the fifth international joint conference on Autonomous agents and multiagent systems*. 810–812.
- [8] Kurt Dresner and Peter Stone. 2005. Multiagent traffic management: Opportunities for multiagent learning. In *International Workshop on Learning and Adaption in Multi-Agent Systems*. Springer, 129–138.
- [9] Samah El-Tantawy, Baher Abdulhai, and Hossam Abdelgawad. 2013. Multiagent reinforcement learning for integrated network of adaptive traffic signal controllers (MARLIN-ATSC): methodology and large-scale application on downtown Toronto. *IEEE Trans. Intelligent Transportation Systems* 14, 3 (2013), 1140–1150.
- [10] Xiaomin Fang, Jizhou Huang, Fan Wang, Lingke Zeng, Haijin Liang, and Haifeng Wang. 2020. ConSTGAT: Contextual Spatial-Temporal Graph Attention Network for Travel Time Estimation at Baidu Maps. In *Proceedings of the 26th ACM SIGKDD International Conference on Knowledge Discovery & Data Mining*. 2697–2705.
- [11] Yazan Abu Farha and Jurgen Gall. 2019. Ms-tcn: Multi-stage temporal convolutional network for action segmentation. In *Proceedings of the IEEE/CVF Conference on Computer Vision and Pattern Recognition*. 3575–3584.
- [12] Rongzhou Huang, Chuyin Huang, Yubao Liu, Genan Dai, and Weiyang Kong. 2020. LSGCN: Long Short-Term Traffic Prediction with Graph Convolutional Networks. In *Proceedings of the Twenty-Ninth International Joint Conference on Artificial Intelligence, IJCAI-20*. International Joint Conferences on Artificial Intelligence Organization, 2355–2361.
- [13] Thomas N Kipf and Max Welling. 2016. Semi-supervised classification with graph convolutional networks. *arXiv preprint arXiv:1609.02907* (2016).
- [14] Nicholas Lim, Bryan Hooi, See-Kiong Ng, Xueou Wang, Yong Liang Goh, Renrong Weng, and Jagannadan Varadarajan. 2020. STP-UDGAT: Spatial-Temporal-Preference User Dimensional Graph Attention Network for Next POI Recommendation. In *Proceedings of the 29th ACM International Conference on Information & Knowledge Management*. 845–854.
- [15] Li Mengzhang and Zhu Zhanxing. 2020. Spatial-Temporal Fusion Graph Neural Networks for Traffic Flow Forecasting. *arXiv preprint arXiv:2012.09641* (2020).
- [16] Abdulllah Mohamed, Kun Qian, Mohamed Elhoseiny, and Christian Claudel. 2020. Social-stgcn: A social spatio-temporal graph convolutional neural network for human trajectory prediction. In *Proceedings of the IEEE/CVF Conference on Computer Vision and Pattern Recognition*. 14424–14432.
- [17] Tomoki Nishi, Keisuke Otaki, Keiichi Hayakawa, and Takayoshi Yoshimura. 2018. Traffic signal control based on reinforcement learning with graph convolutional neural nets. In *2018 21st International Conference on Intelligent Transportation Systems*. IEEE, 877–883.
- [18] Zhen Peng, Wenbing Huang, Minnan Luo, Qinghua Zheng, Yu Rong, Tingyang Xu, and Junzhou Huang. 2020. Graph representation learning via graphical mutual information maximization. In *Proceedings of The Web Conference 2020*. 259–270.
- [19] Roger P Roess, Elena S Prassas, and William R McShane. 2004. *Traffic engineering*. Pearson/Prentice Hall.
- [20] Emanuele Rossi, Ben Chamberlain, Fabrizio Frasca, Davide Eynard, Federico Monti, and Michael Bronstein. 2020. Temporal graph networks for deep learning on dynamic graphs. *arXiv preprint arXiv:2006.10637* (2020).
- [21] Aravind Sankar, Yanhong Wu, Liang Gou, Wei Zhang, and Hao Yang. 2018. Dynamic graph representation learning via self-attention networks. *arXiv preprint arXiv:1812.09430* (2018).
- [22] Leena Singh, Sudhanshu Tripathi, and Himakshi Arora. 2009. Time optimization for traffic signal control using genetic algorithm. *International Journal of Recent Trends in Engineering* 2, 2 (2009), 4.
- [23] Rakshit Trivedi, Mehrdad Farajtabar, Prasenjeet Biswal, and Hongyuan Zha. 2019. Dyrep: Learning representations over dynamic graphs. In *International Conference on Learning Representations*.
- [24] Bhattacharya Uttaran, Mittal Trisha, Chandra Rohan, Randhavane Tanmay, Bera Aniket, and Manocha Dinesh. 2020. STEP: Spatial Temporal Graph Convolutional Networks for Emotion Perception from Gaits. In *Proceedings of the AAAI Conference on Artificial Intelligence*, Vol. 34. 1342–1350.
- [25] Aaron van den Oord, Dieleman Sander, Zen Heiga, Simonyan Karen, Vinyals Oriol, Graves Alex, Kalchbrenner Nal, Senior Andrew, and Kavukcuoglu Koray. 2016. WaveNet: A Generative Model for Raw Audio. *arXiv preprint arXiv:1609.03499* (2016).
- [26] Elise Van der Pol and Frans A Oliehoek. 2016. Coordinated deep reinforcement learners for traffic light control. *Proceedings of Learning, Inference and Control of Multi-Agent Systems (at NIPS 2016)* (2016).
- [27] Pravin Varaiya. 2013. The max-pressure controller for arbitrary networks of signalized intersections. In *Advances in Dynamic Network Modeling in Complex Transportation Systems*. Springer, 27–66.
- [28] Petar Veličković, Guillem Cucurull, Arantxa Casanova, Adriana Romero, Pietro Lio, and Yoshua Bengio. 2017. Graph attention networks. *arXiv preprint arXiv:1710.10903* (2017).
- [29] Hua Wei, Nan Xu, Huichu Zhang, Guanjie Zheng, Xinshi Zang, Chacha Chen, Weinan Zhang, Yanmin Zhu, Kai Xu, and Zhenhui Li. 2019. Colight: Learning network-level cooperation for traffic signal control. In *Proceedings of the 28th ACM International Conference on Information and Knowledge Management*. 1913–1922.
- [30] Hua Wei, Guanjie Zheng, Vikash Gayah, and Zhenhui Li. 2019. A survey on traffic signal control methods. *arXiv preprint arXiv:1904.08117* (2019).
- [31] Hua Wei, Guanjie Zheng, Huaxiu Yao, and Zhenhui Li. 2018. Intellilight: A reinforcement learning approach for intelligent traffic light control. In *Proceedings of the 24th ACM SIGKDD International Conference on Knowledge Discovery & Data Mining*. 2496–2505.
- [32] Kok-Lim Alvin Yau, Junaid Qadir, Hooi Ling Khoo, Mee Hong Ling, and Peter Komisarczuk. 2017. A survey on reinforcement learning models and algorithms for traffic signal control. *ACM Computing Surveys (CSUR)* 50, 3 (2017), 1–38.
- [33] Xinshi Zang, Huaxiu Yao, Guanjie Zheng, Nan Xu, Kai Xu, and Zhenhui Li. 2020. MetaLight: Value-Based Meta-Reinforcement Learning for Traffic Signal Control. In *Proceedings of the AAAI Conference on Artificial Intelligence*, Vol. 34. 1153–1160.
- [34] Huichu Zhang, Siyuan Feng, Chang Liu, Yaoyao Ding, Yichen Zhu, Zihan Zhou, Weinan Zhang, Yong Yu, Haiming Jin, and Zhenhui Li. 2019. Cityflow: A multi-agent reinforcement learning environment for large scale city traffic scenario. In *The World Wide Web Conference*. 3620–3624.
- [35] Shijie Zhang, Hongzhi Yin, Tong Chen, Quoc Viet Nguyen Hung, Zi Huang, and Lizhen Cui. 2020. GCN-Based User Representation Learning for Unifying Robust Recommendation and Fraudster Detection. In *Proceedings of the 43rd International ACM SIGIR Conference on Research and Development in Information Retrieval*. 689–698.
- [36] Xiyue Zhang, Chao Huang, Yong Xu, and Lianghao Xia. 2020. Spatial-Temporal Convolutional Graph Attention Networks for Citywide Traffic Flow Forecasting. In *Proceedings of the 29th ACM International Conference on Information & Knowledge Management*. 1853–1862.
- [37] Guanjie Zheng, Yuanhao Xiong, Xinshi Zang, Jie Feng, Hua Wei, Huichu Zhang, Yong Li, Kai Xu, and Zhenhui Li. 2019. Learning phase competition for traffic signal control. In *Proceedings of the 28th ACM International Conference on Information and Knowledge Management*. 1963–1972.